

Angular dependence of giant magnetoimpedance in an amorphous Co-Fe-Si-B ribbon

K. R. Pirota, L. Kraus,* M. Knobel, P. G. Pagliuso, and C. Rettori
*Instituto de Física "Gleb Wataghin," Universidade Estadual de Campinas (UNICAMP), C.P. 6165,
 Campinas 13083-970, São Paulo, Brazil*

(Received 8 March 1999)

The field response of impedance is studied in a stress-annealed amorphous ribbon as a function of the angle of application of the external magnetic field in order to verify the role of induced anisotropies (and their distribution) and demagnetizing factors in the giant magnetoimpedance (GMI) phenomenon which occurs in soft magnetic materials. The experimental results are well explained by a theoretical model, based on the simultaneous solution of Maxwell equations and the Landau-Lifshitz equation of motion. Demagnetizing effects are properly taken into account in the case of ribbons or thin films. The physical parameters necessary to test the theory were obtained through complementary measurements of the ferromagnetic resonance and temperature dependence of magnetization. The results clearly indicate the enormous influence of the distribution of anisotropies on the GMI effect. Also, an experimental procedure for determining the easy-axis distribution function is proposed. [S0163-1829(99)15433-X]

I. INTRODUCTION

Recent research concerning the field and frequency response of impedance in soft magnetic conductors has unveiled a new and fascinating phenomenon, known as giant magnetoimpedance (GMI). Strong and sensitive field-induced variations of the impedance were first observed in amorphous wires¹ and ribbons,² and later in nanocrystalline materials (wires³ and ribbons⁴) and soft magnetic thin films.⁵ A major role in GMI is played by the skin depth δ , the square of which is directly proportional to the resistivity of the material and inversely proportional to the transversal permeability and frequency of the probe current.⁶ Soft magnetic materials display very large magnetic permeabilities, which are strongly affected by relatively small magnetic fields. These changes are immediately reflected in δ and, therefore, in the impedance of the material considered. Although GMI was discovered quite recently, it has been studied intensively, mainly owing to the great possibilities for technological applications. Also, even if the basic aspects of the phenomenon can be qualitatively understood in terms of classical electrodynamics, systematic investigation has revealed several experimental results which remain to be clarified. For example, it is well known that inducing transverse anisotropies contributes to a significant increase of the GMI ratios, which, however, usually occurs with the appearance of new features, such as definite peak structures^{5,7} and hysteretic behavior.⁸ Only recently, with the further development of theoretical models, which now include the dynamics of magnetization rotation through the Landau-Lifshitz equation of motion⁹ and take into account the exchange effects,^{10,11} has the study of the effect of anisotropies on the GMI behavior become feasible.

Hitherto, most studies of GMI effect concentrated on the longitudinal magnetoimpedance (LMI), in which the external magnetic field is applied along the direction of the probe current I . LMI in amorphous and nanocrystalline materials with well-defined magnetic anisotropy usually exhibits either a single- or double-peak structure, for the easy axis parallel or perpendicular to the current direction, respectively.¹² Little work on magnetoimpedance with external field applied

perpendicular to the current direction has been reported.^{5,14-17} In ribbons or thin films two additional geometries can be distinguished: transverse magnetoimpedance (TMI) for the field in the ribbon plane^{5,13,16} or perpendicular magnetoimpedance (PMI) for the field perpendicular to it.^{13,14,16} While the behavior of LMI is relatively well understood, the TMI and PMI results are rather confusing and not well understood. An observation of TMI was reported by Sommer and Chien in amorphous $\text{Fe}_{73.5}\text{CuNb}_3\text{Si}_{13.5}\text{B}_9$ thin films.⁵ For the transversely field annealed sample they observed a relatively strong GMI effect in both LMI and TMI configurations in similar field ranges. The main difference was the single- and double-peak structure for TMI and LMI, respectively.⁵ Similarity in the magnitude, field range, and frequency behavior of LMI and TMI has been also observed in crystalline NiFe and amorphous NiCoFeMnSiB melt extracted fibers.¹⁵ On the contrary, LMI, TMI, and PMI measurements in low magnetostrictive amorphous ribbons show similarly large effects, but with different peak structures and in substantially different field ranges depending upon the corresponding demagnetizing factor.^{13,14} Recently reported LMI, TMI, and PMI measurements on amorphous FeNiCrSiB films, annealed above the Curie temperature, show similar magnitudes of GMI, but only the single-peak behavior in all the three possible configurations.¹⁶

In this paper we investigate the GMI effect as a function of the angle of application of the external magnetic field in stress-annealed amorphous ribbons in order to verify the role of induced anisotropies (and their distribution) and demagnetizing factors in the impedance response of soft magnetic samples. In addition to the clues that these experiments furnish for the fundamental framework of magnetoimpedance phenomena, they are also important in view of possible applications of GMI elements as nonfixed magnetic sensors, where the field can be applied in any spatial direction.

II. EXPERIMENTAL DETAILS

Our experiments were performed on an $(\text{Fe}_{0.053}\text{Co}_{0.947})_{70}\text{Si}_{12}\text{B}_{18}$ amorphous ribbon (width 0.8 mm,

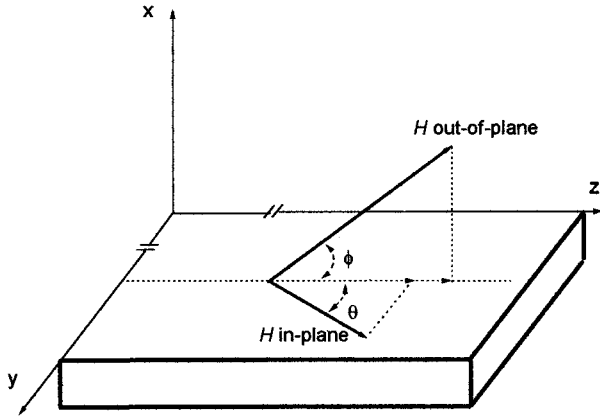


FIG. 1. Geometric configuration of the experiment. In this figure one can see the ribbon plane and the two possible angles of application of the external magnetic field. The current was applied in the Z direction.

thickness $22 \mu\text{m}$). The sample was submitted to preannealing for 1 h at 360°C followed by 1 h stress annealing at 340°C (applied tensile stress of 400 MPa).¹⁸ This thermal treatment produced a shift of the saturation magnetostriction constant λ_s , which acquired a small but negative value (-1×10^{-8}) after the annealing procedure. Furthermore, the thermal treatment induced a well-defined magnetic anisotropy perpendicular to the ribbon axis, as previously reported,¹⁸ and confirmed through Kerr effect observations of the domain structure.

The impedance was measured in both as-quenched and stress-annealed samples using an experimental setup described elsewhere.¹⁹ The ribbon strips were typically 10 cm long, and the contacts were made with silver paint 8 cm apart, and typically had 1Ω resistance. The field response of the impedance was measured with a lock-in amplifier for different frequencies (up to 900 kHz) of the probe current I (up to 8 mA). The ribbon strips were positioned on a rotatable table in a Helmholtz coil system, which supplies the external dc magnetic field (up to 100 Oe). This rotatable table allowed us to apply the external magnetic field in different directions specified in Fig. 1, including out-of-plane fields (angle ϕ) and in-plane fields (angle θ).

It is worth noting that the sample studied is an extremely soft magnetic material and that really small magnetic fields can modify its behavior significantly. Because we were not working in a shielded room and we did not have Earth's field compensation, extensive data analysis had to be performed in order to make subtle corrections in the experimental results. Despite positioning the Helmholtz pair axis perpendicular to Earth's magnetic field, we always had to deal with a stray magnetic field from the environment. By analyzing the peak positions and their asymmetry in the GMI curves, it was possible to estimate the real magnetic field and its angle of application by performing simple vector calculations.

In order to estimate the transverse demagnetizing factor of the ribbon and to determine the Gilbert damping parameter, a ferromagnetic resonance (FMR) experiment was performed at room temperature. It was measured at the microwave frequency of 9.32 GHz on a 1.7-cm-long, as-quenched, sample with magnetic field applied in the ribbon plane in both the parallel and transverse directions. The resulting resonance

spectra are rather asymmetric, probably owing to the surface roughness of the samples. However, from the difference of the resonance fields in the parallel and transverse configurations, it is possible to extract valuable information about the transverse demagnetizing factor (N_y), which, from our results, turns out to lie between 0.014 and 0.019. Also, from the resonance linewidth (138 Oe), it was possible to estimate the Gilbert damping parameter $\alpha = 2.7 \times 10^{-2}$. It is important to stress that this is obviously an overestimation of α , because of possible extra broadening of the line due to some anisotropy distribution or surface roughness of the sample.

The exchange stiffness constant $A = 3 \times 10^{-12} \text{ J/m}$ was obtained from the Bloch law²⁰ through the temperature dependence of saturation magnetization (from 2 to 300 K) measured in a Quantum Design PPMS system.

III. THEORETICAL BACKGROUND

At high frequencies, the ac permeability of ferromagnetic metals is controlled mainly by magnetization rotation process. Due to the large eddy current damping,²¹ the contribution of domain wall motion can be neglected. This fact makes the theoretical analysis of GMI effect at high frequencies somewhat easier.

The phenomenological theory of GMI is based on simultaneous solution of Maxwell's equations and the Landau-Lifshitz equation of motion.^{11,22} The magnitude of GMI, calculated for a semi-infinite film with an in-plane uniaxial anisotropy, is extremely high if the internal dc field \mathbf{H}_0 satisfies the FMR resonance condition²²

$$H_0 \cos \theta \approx H_K \cos 2(\theta + \psi) + \frac{1}{M_s} \left(\frac{\omega}{\gamma} \right)^2, \quad (1)$$

where H_K is the anisotropy field, M_s the saturation magnetization, ω the angular frequency of the driving current, γ the spectroscopic splitting factor, and ψ the angle between \mathbf{H}_0 and the hard anisotropy axis. The equilibrium angle between the internal field and dc magnetization vector, θ , can be calculated from the equation

$$2H_0 \sin \theta = H_K \sin 2(\theta + \psi). \quad (2)$$

For small frequencies of driving current [$(\omega/\gamma)^2 \ll M_s H_K$], the resonance condition (1) can be fulfilled only if $\psi = 0$ and $H_0 \approx H_K$. If the magnitude of internal field \mathbf{H}_0 differs from H_K and its direction deviates from the hard anisotropy axis, the theoretical magnitude of impedance sharply decreases. This is illustrated in Fig. 2, where the modulus of relative impedance calculated for a film with typical parameters of our stress-annealed sample ($J_s = 0.6 \text{ T}$, $H_K = 520 \text{ A/m} = 6.5 \text{ Oe}$, $g = 2.1$, $\alpha = 0.027$, $\rho = 1.22 \mu\Omega \text{ m}$, $A = 3 \times 10^{-12} \text{ J/m}$, and $t = 13.7 \mu\text{m}$), at the driving frequency of 500 kHz, is shown. The direction of the easy anisotropy axis, described by the unit vector \mathbf{n} , was chosen to lie in the film plane and make an angle of 60° with the direction of the driving current (z axis). The function $|Z|/R_{\text{dc}}$, where R_{dc} is the dc resistance, plotted as a function of the y and z components of internal field \mathbf{H}_0 , exhibits a sharp ridge along the hard axis and a sharp peak at $H_0 = H_K$. The dispersion of easy axis \mathbf{n} or anisotropy field H_K in real materials leads to smearing of the peak and to a de-

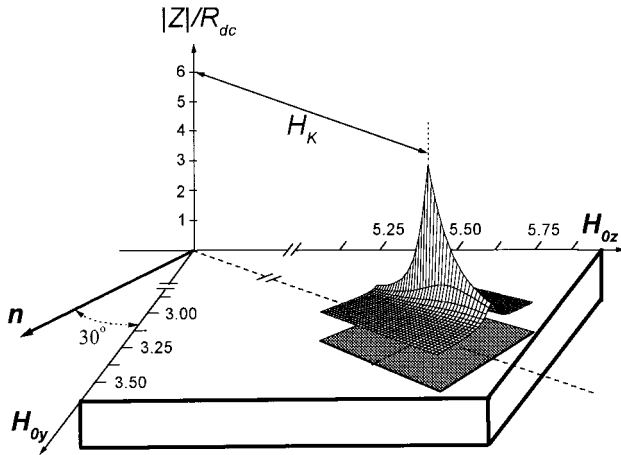


FIG. 2. Modulus of relative impedance divided by the dc resistance calculated for a film with the parameters $J_s = 0.6$ T, $H_K = 520$ A/m = 6.5 Oe, $g = 2.1$, $\alpha = 0.027$, $\rho = 1.22 \mu\Omega$ m, $A = 3 \times 10^{-12}$ J/m, $t = 13.7 \mu\text{m}$, and $f = 500$ kHz. Here the easy axes make an angle of 60° with the current direction (ribbon axis). The field units are plotted in Oe.

crease of its height.²² In the following, the shape of actual GMI curves will be estimated. Only the dispersion of the easy axis in the film plane (y, z) will be considered, for simplicity.

First, let us define the vector $\mathbf{H}_K = H_K \mathbf{e}_x \times \mathbf{n}$, which has the length H_K and the direction of the hard axis in the film plane. Thus the modulus of the relative complex impedance $F(\mathbf{H}_0, \mathbf{H}_K) = Z/R_{dc}$ has a sharp peak for $\mathbf{H}_0 = \mathbf{H}_K$. Let us suppose that the contributions of elementary volumes, where the field \mathbf{H}_K can be considered homogeneous, to the total impedance are independent of each other. If all the elements are assumed to be connected in series, the total impedance of the sample can be calculated from the formula

$$Z(\mathbf{H}_0) = \int F(\mathbf{H}_0, \mathbf{H}_K) p(\mathbf{H}_K) dH_{Ky} dH_{Kz}, \quad (3)$$

where the distribution function $p(\mathbf{H}_K)$ characterizes the fluctuation of anisotropy in the y, z plane. If the peak of the function $F(\mathbf{H}_0, \mathbf{H}_K)$ at $\mathbf{H}_0 = \mathbf{H}_K$ is much sharper than the variation of $p(\mathbf{H}_K)$, then in Eq. (3) the function F can be replaced roughly by $F_{\max}(\mathbf{H}_0) \delta(\mathbf{H}_0 - \mathbf{H}_K)$, where $F_{\max}(\mathbf{H}_0) = F(\mathbf{H}_0, \mathbf{H}_0)$ is the maximum theoretical value of Z/R_{dc} . One then obtains

$$Z(\mathbf{H}_0) \approx F_{\max}(\mathbf{H}_0) p(\mathbf{H}_0). \quad (4)$$

Because the modulus of $F_{\max}(\mathbf{H}_0)$ depends only slightly on the field \mathbf{H}_0 ,²² the distribution of anisotropy fields in the film plane can be investigated by measuring the function $|Z(\mathbf{H}_0)|$ with various orientations of the internal field \mathbf{H}_0 .

When using Eq. (4) for ribbon samples, one has to consider the demagnetizing effect of the sample edges. Because the flux of the ac field, produced by the probe current, is closed around the ribbon edges, the ac demagnetizing field can be neglected. If, however, the external dc field \mathbf{H} is not exactly parallel to the ribbon axis, the magnetic charges appearing on the sample surfaces produce a transverse dc demagnetizing field \mathbf{H}_d . Then the internal field \mathbf{H}_0 , appearing

in Eq. (4), is $\mathbf{H}_0 = \mathbf{H} + \mathbf{H}_d$. For the external field applied in the y, z plane, the impedance as a function of external field is given by

$$Z(H_y, H_z) \approx F_{\max} p(H_y - N_y M_y, H_z), \quad (5)$$

where N_y is the transverse demagnetizing factor and M_y the transverse magnetization of the ribbon. If the demagnetizing factor were known and the transverse magnetization were measured, the distribution function $p(H_{Ky}, H_{Kz})$ could be reconstructed from the angular dependence of the GMI effect. Unfortunately, it is rather difficult to measure the transverse component of magnetization in samples with a high aspect ratio.

However, for the ribbon with a well-defined transverse anisotropy, the transverse demagnetizing field may be roughly estimated. Because the transverse magnetization process is controlled mainly by domain wall movement, we can assume nearly ideally soft behavior in the y direction. The transverse component of magnetization is then given by $M_y \approx H_y / N_y$ for $|H_y| < N_y M_s$, and by $M_y \approx M_s$ for $|H_y| > N_y M_s$. The transverse component of internal magnetic field is then

$$H_{0y} = H_y - N_y M_y \approx \begin{cases} 0 & \text{for } |H_y| < N_y M_s, \\ H_y - N_y M_s & \text{for } H_y > N_y M_s. \end{cases} \quad (6)$$

For well-defined transverse anisotropy (i.e., easy axis in the y direction), the distribution function $p(\mathbf{H}_0)$ has a distinct maximum at $\langle \mathbf{H}_K \rangle = (0, \langle H_K \rangle)$. If the external field \mathbf{H} is applied in the ribbon plane at an angle θ with respect to the z axis, then according to Eqs. (5) and (6) the GMI curve exhibits maxima at $H \approx \pm \langle H_K \rangle / \cos \theta$ for $H \sin \theta < N_y M_s$. For $H \sin \theta > N_y M_s$, the maxima should shift to higher values of H and their heights should decrease.

IV. RESULTS AND DISCUSSION

A. Longitudinal magnetoimpedance

Systematic measurements of giant magnetoimpedance and its relaxation [magnetoimpedance aftereffect (MIAE)] were previously performed on a series of Co-rich amorphous ribbons with slightly different compositions and hence different magnetostriction constants λ_s .²³ The stress annealing, used to produce the transverse magnetic anisotropy, also causes a modification of magnetostriction constant. The behavior of GMI changes drastically upon stress annealing. The as-quenched samples exhibit maximum impedance at zero applied field and a monotonic decrease with increasing longitudinal applied field. After stress annealing, all samples display a hysteretic behavior and a well-defined peak structure, but the magnitude of the maximum impedance is not much affected by the thermal treatment. The impedance relaxation (aftereffect) is strongly suppressed after the annealing procedure.²³

Figure 3(a) shows the relative quantity Z/R_{dc} for the stress-annealed sample. The measurement was performed with a probe current amplitude of 5 mA at frequencies of 100, 500, and 900 kHz. In Fig. 3(b) the relative impedance modulus for probe current amplitudes of 1, 5, and 8 mA at a fixed frequency of 900 kHz is shown. The configuration used here was the LMI, with the field applied along the ribbon

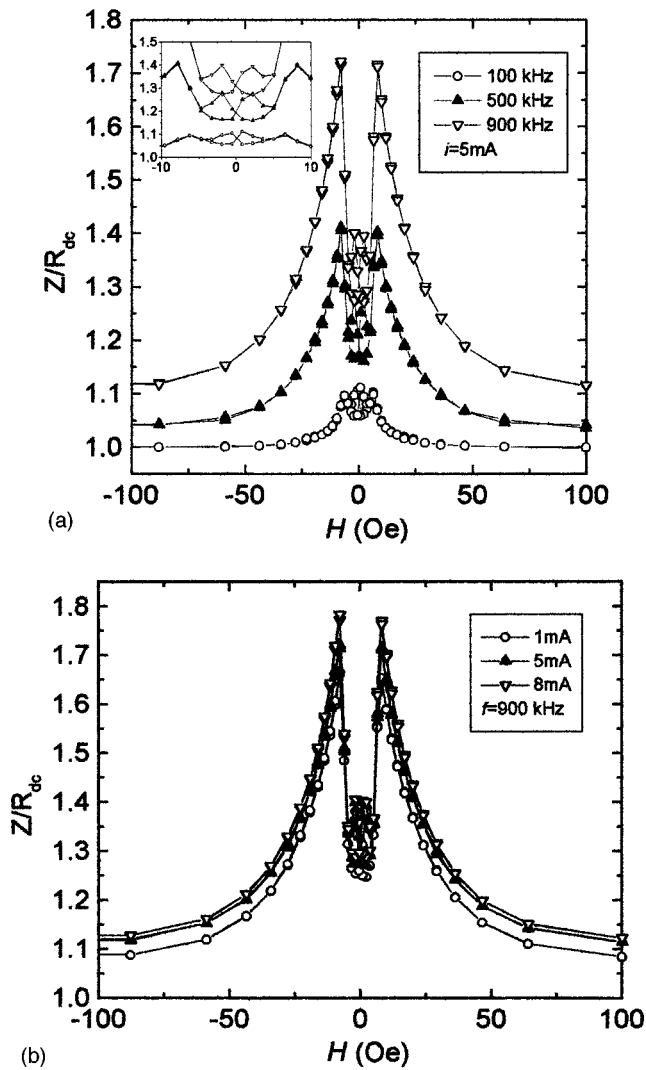


FIG. 3. (a) Ratio Z/R_{dc} for the stress-annealed sample as a function of the longitudinally applied magnetic field. Probe current amplitude $I=5$ mA and frequencies: \circ (100 kHz), \blacktriangle (500 kHz), and ∇ (900 kHz). The inset shows the central hysteretic behavior in more detail. (b) Ratio Z/R_{dc} for a fixed probe current frequency of 900 kHz and different current intensities: \circ (1 mA), \blacktriangle (5 mA), and ∇ (8 mA).

axis (z axis in Fig. 1). The peaks in GMI are positioned at about ± 9 Oe (very close to the anisotropy field H_K measured from the hysteresis loop²³). Such peaks, which are not observed in the as-quenched sample, are related to the transverse anisotropy induced by the stress annealing.^{9,24–26} The small asymmetry observed in the peak height is probably caused by a stray magnetic field.

Besides possible changes of the transverse permeability, the annealing can have an enormous influence on the distribution of anisotropy fields within the sample and, consequently, on the longitudinal magnetoimpedance. Sommer and Chien concluded that only the transverse component of the magnetic anisotropy contributes to the LMI.²⁴ However, notice that for 500 kHz the maximum ratio Z/R_{dc} is approximately 1.4, although our theoretical model²² predicts ratios of the order of 6. Taking into account the numerous approximations used in the model, this discrepancy is still large, and

it is a clear indication that the anisotropy is not perfectly uniaxial. Indeed, in the real sample there is a distribution of anisotropy axes, which gives rise to a drastic decrease of the idealized magnetoimpedance peak.

A weaker peak structure possessing hysteretic behavior can also be clearly seen on the inner part of the GMI curve [see inset in Fig. 3(a)]. The maxima can be observed only for $H < 0$ on the decreasing branch and for $H > 0$ on the increasing branch of the curve. Such peaks are present in all annealed samples and seem to be related to the coercive field of small hysteresis loops superimposed on the nonhysteretic magnetization curves typical for purely rotational magnetization processes. Similar effects have previously been observed for other magnetic systems.^{24,27–29} Sinnecker *et al.*⁸ ascribed them to irreversible domain wall displacements at fields smaller than the anisotropy field H_K . Although several authors have extensively observed this behavior, which is evidently connected with the domain structure, there is not yet a clear explanation of its origin. The application of the external magnetic fields at different angles provokes a clear expansion of the field range where the hysteretic effect occurs (see next section), indicating that this behavior is certainly related to irreversible magnetization processes of a particular domain configuration. The dilation of the range where the effect occurs can, in principle, facilitate further experiments to clarify this point.

When the frequency of the probe current is increased, the maximum change of impedance with applied field also increases. The frequency dependence of LMI may be understood in terms of the frequency dependence of the skin depth δ .⁶ The dependence of Z on the amplitude of probe current also depends on the frequency. The magnitude of LMI generally increases with current amplitude,²³ but for high frequencies (900 kHz) the influence of current amplitude on magnetoimpedance seems to vanish. More details on this behavior of magnetoimpedance are discussed in Ref. 23. Once the properties of impedance spectra in the longitudinal configuration had been well established, the fixed amplitude of 1 mA and the frequency of 500 kHz were used to study the effect of magnetic field orientation on the giant magnetoimpedance effect.

B. In-plane field

Figure 4 shows the field dependence of the impedance Z measured for magnetic fields applied in the ribbon plane at different angles θ with the ribbon axis. The maximum applied field was chosen so that the most important features were seen on all the curves, if possible. For low θ values the external field was limited to ± 20 Oe and was increased up to ± 100 Oe (near the limit of our system) for angles close to 90° . Hysteretic behavior is clearly observed on all curves. The position of the peaks shifts towards higher values with increasing θ and goes beyond the available field range for $\theta \approx 90^\circ$. For $\theta = 88^\circ$ the impedance curve becomes nearly flat, as expected from theoretical calculations. Figure 5 shows the same data as in Fig. 4 plotted as a function of $(H-a)\cos\theta$, which represents the z component of internal magnetic field H_{0z} . A correction constant $a = 1.0$ Oe, common to all curves, was obtained by the fit of data to account for the residual magnetic field. As expected from the theory,

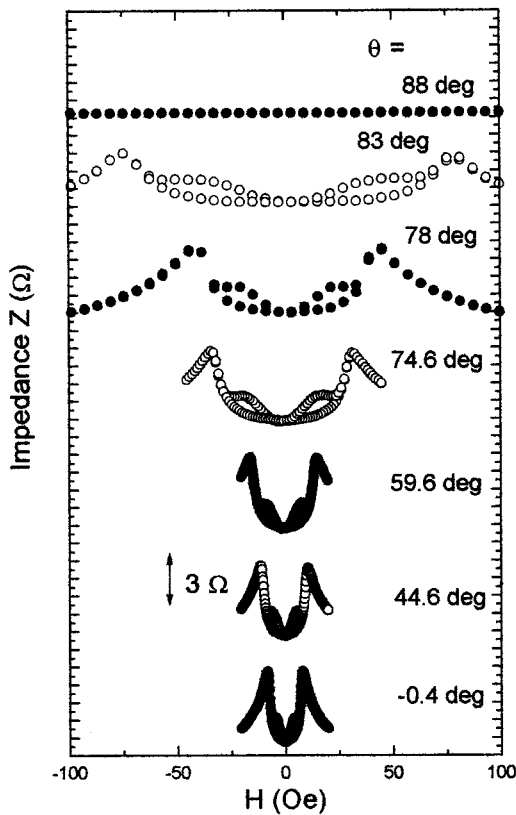


FIG. 4. Field dependence of impedance Z for a magnetic field applied in the plane of the ribbon at different angles θ , where θ is the angle between the applied field and the ribbon axis (current direction).

all curves become similar after this rescaling. The maxima now appear at ± 8.8 Oe, which corresponds well to the transverse anisotropy field determined from the hysteresis loop.

The behavior of GMI in the stress-annealed sample satisfies the theoretical predictions for the ribbon with a well-defined transverse anisotropy. Because the shape and magnitude of the “normalized” GMI curves does not depend on the angle for $\theta \leq 83^\circ$ it seems to be determined only by the distribution function $p(0, H_{Kz})$. This means that the y component of internal field H_{0y} is equal to zero. For ideal magnetic softness in the y direction, this can happen for $H \sin \theta < N_y M_s$. From the transverse demagnetizing factor measured by FMR, one obtains $N_y M_s$ in the range from 84 to 114 Oe, which is close to the maximum field available in our equipment.

An interesting experimental comment is important here. The present experiments demonstrate how sensitive these soft magnetic samples are not only to the presence of magnetic stray fields, but also to the angle of application of external magnetic fields. When dealing with these materials, extreme care must be taken in order to apply a well-determined field at the correct angle. Small deviations in the angle of application of the field can cause strong variations on the impedance response (see Fig. 4, for example).

Comparing our results with those obtained by Sommer and Chien,^{5,13} it is worth noting that our impedance curves have a simpler hysteretic behavior and a better defined (and simpler) peak structure. Sommer and Chien also observed broad bell-shaped curves in the TMI configuration, which do

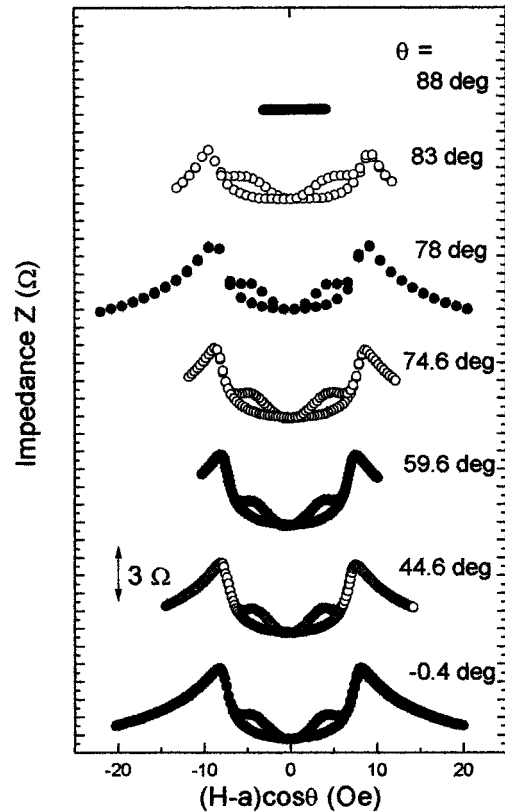


FIG. 5. Impedance modulus Z for a magnetic field applied in the ribbon plane plotted as a function of the z component (ribbon axis) of internal magnetic field H_{0z} . The small correction constant to account for the residual magnetic field was $a = 1.0$ Oe.

not appear in our experiment. These differences possibly indicate that the samples used in their study have a broad distribution of anisotropies (easy axis), even after field annealing. It is also important to note that when the experiments are performed at lower frequencies¹³ there is an extra contribution of the domain wall movements to the overall magnetization process, and theoretical analysis becomes extremely complicated.

C. Out-of-plane field

In this case the specimen was placed on the rotatable table so that the axis of rotation was in the ribbon plane, transverse to the ribbon axis (in the y axis; see Fig. 1). The field dependence of complex impedance was measured for different out-of-plane angles ϕ (see Fig. 1). Figure 6 shows the field dependence of Z obtained for a drive current of 1 mA at 500 kHz. In these measurements, special care was taken to apply the field exactly in the x - z plane; i.e., the projection of applied field in the y direction was always negligible with respect to its z component ($\theta = 0^\circ$).

It can be seen that the position of the GMI peaks shifts towards larger values with increasing ϕ , surpassing our maximum field for angles above 85° . Similarly as in the in-plane case, the impedance curves become nearly flat for $\phi \approx 90^\circ$ (perpendicular GMI). The normalized field dependence, corrected by the constant offset a (still 1 Oe) and multiplied by the factor $\cos \phi$, is shown in Fig. 7. All curves again become similar after the geometric effects are taken

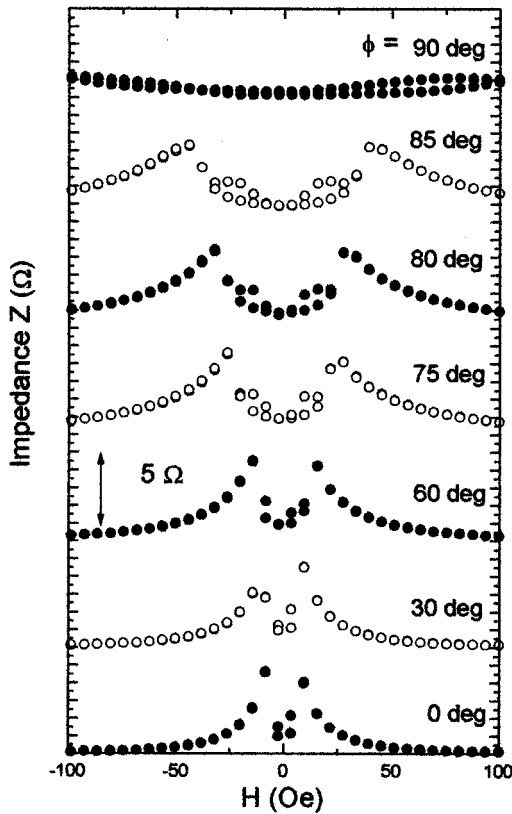


FIG. 6. Field dependence of impedance Z for a magnetic field applied out of the plane of the ribbon at different angles ϕ , where ϕ is the angle between the applied field and the ribbon axis (see Fig. 1).

into account. The perpendicular anisotropy field appears approximately in the position 8.2 Oe.

In the theoretical discussion, the out-of-plane orientation of magnetic field was not considered. Nevertheless, the theoretical conclusions can also be used for this experimental configuration. This is probably because the normal demagnetizing factor N_z of the ribbon, which is close to 1, strongly suppresses the out-of-plane component of magnetization for the applied fields used in these experiments.

V. CONCLUSIONS

A theoretical model has been presented to explain the magnetoimpedance response of films or ribbons with well-defined uniaxial anisotropy for magnetic fields applied at arbitrary angles (in the film or ribbon plane). Considering samples with a distribution of easy axes, it was possible to use the model (with some approximations) to predict the expected experimental behavior.

On the experimental side, longitudinal magnetoimpedance was studied as a function of the frequency and amplitude of the probe current. Some indications of the influence of anisotropy distribution within the samples were obtained by comparing the experimental results with the theoretical values expected for an ideal uniaxial anisotropy. The investigation of the GMI effect in the stress-annealed amorphous ribbon with an oblique orientation of the applied magnetic field has shown the enormous influence of the distribution of anisotropies and demagnetizing factor on GMI. The experi-

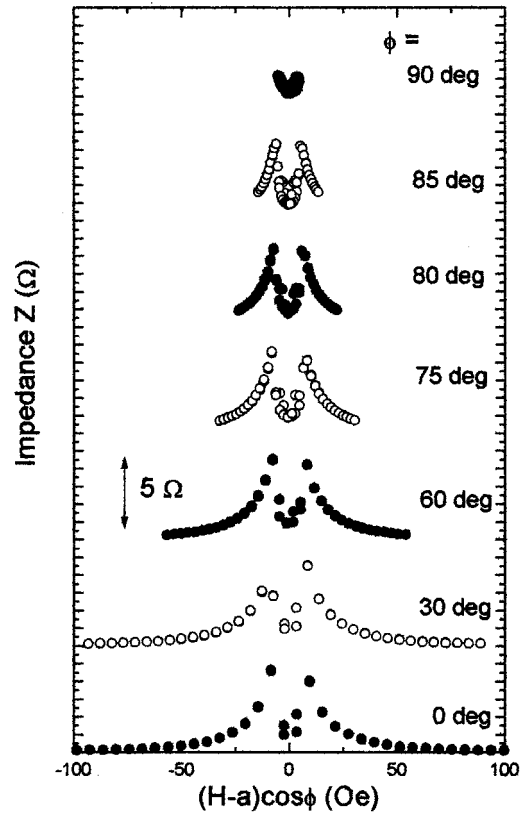


FIG. 7. Same as Fig. 5, for magnetic fields applied out of the plane of the ribbon.

mental results obtained for a ribbon with a well-defined transverse magnetic anisotropy could be easily understood in terms of the proposed theoretical model. The theoretical analysis indicates that the distribution of magnetic anisotropy in the sample could be inferred from this kind of experiment if the demagnetizing fields were determined by independent measurements.

Although our experimental setup did not allow the application of higher magnetic fields, it was possible to extract valuable information about the anisotropy distribution of our sample and the effect of the geometry of the application of the external fields. In light of these results, it is clear that more systematic measurements of impedance, as a function of the angle of application of the field and its intensity, are necessary in order to explain the few results found in the literature. These experiments, if properly analyzed, can provide a valuable technique to determine the anisotropy distribution in amorphous ribbons and thin films. Also, the present theoretical and experimental results can be very useful in view of future applications of GMI elements as nonfixed magnetic sensors, where the external magnetic field can be applied in arbitrary spatial directions.

ACKNOWLEDGMENTS

The authors express their gratitude to J. Gutierrez and J. M. Barandiarán (Bilbao) for providing the samples and to L. Melo and A. D. dos Santos (São Paulo) for the Kerr effect experiment. CNPq and FAPESP (Brazilian agencies) financially supported this work.

- *Permanent address: Institute of Physics, ASCR, Na Slovance 2, CZ-182 21 Praha 8, Czech Republic.
- ¹R. S. Beach and A. E. Berkowitz, *Appl. Phys. Lett.* **64**, 3652 (1994).
- ²F. L. A. Machado, B. L. da Silva, S. M. Rezende, and C. S. Martins, *J. Appl. Phys.* **75**, 6563 (1994).
- ³M. Knobel, M. L. Sánchez, C. Gómez-Polo, A. Hernando, P. Marín, and M. Vázquez, *J. Appl. Phys.* **79**, 1646 (1996).
- ⁴M. Knobel, J. Schoenmaker, J. P. Sinnecker, R. Sato Turtelli, R. Grössinger, W. Hofstetter, and H. Sassik, *Mater. Sci. Eng., A* **226-228**, 546 (1997).
- ⁵R. L. Sommer and C. L. Chien, *Appl. Phys. Lett.* **67**, 3346 (1995).
- ⁶L. D. Landau and E. M. Lifshitz, *Electrodynamics of Continuous Media* (Pergamon, Oxford, 1975), p. 195.
- ⁷F. L. A. Machado, C. S. Martins, and S. M. Rezende, *Phys. Rev. B* **51**, 3926 (1995); L. V. Panina and K. Mohri, *Appl. Phys. Lett.* **65**, 1189 (1994).
- ⁸J. P. Sinnecker, P. Tiberto, G. V. Kurlyandskaya, E. H. C. Sinnecker, M. Vázquez, and A. Hernando, *J. Appl. Phys.* **84**, 5814 (1998).
- ⁹L. V. Panina, K. Mohri, T. Uchiyama, M. Noda, and K. Bushida, *IEEE Trans. Magn.* **MAG-31**, 1249 (1995).
- ¹⁰A. Yelon, D. Ménard, M. Britel, and P. Ciureanu, *Appl. Phys. Lett.* **69**, 3084 (1996).
- ¹¹D. Menard, M. Britel, P. Ciureanu, and A. Yelon, *J. Appl. Phys.* **84**, 2805 (1998).
- ¹²M. Knobel, *J. Phys. IV* **PR2**, 213 (1998).
- ¹³R. L. Sommer and C. L. Chien, *Phys. Rev. B* **53**, R5982 (1996).
- ¹⁴K. C. Mendes, F. L. A. Machado, L. G. Pereira, S. M. Rezende, F. C. Montenegro, M. V. P. Altoé, and F. P. Missel, *J. Appl. Phys.* **79**, 6555 (1996).
- ¹⁵P. Ciureanu, P. Rudkowski, G. Rudkowska, D. Menard, M. Britel, J. F. Currie, J. O. Ström-Olsen, and A. Yelon, *J. Appl. Phys.* **79**, 5136 (1996).
- ¹⁶S. Q. Xiao, Y. H. Liu, L. Zhang, C. Chen, J. X. Lou, S. X. Zhou, and G. D. Liu, *J. Phys.: Condens. Matter* **10**, 3651 (1998).
- ¹⁷L. Kraus, A. N. Medina, F. G. Gandra, M. Knobel, and V. Haslar, *Mater. Sci. Forum* **302-303**, 224 (1999).
- ¹⁸O. V. Nielsen, J. R. Petersen, B. Hernando, J. Gutierrez, and F. Primdhal, *An. Fis., Ser. B* **86**, 271 (1990).
- ¹⁹J. P. Sinnecker, M. Knobel, M. L. Sartorelli, and J. Schoenmaker, *J. Phys. IV* **PR2**, 665 (1998).
- ²⁰T. Kaneyoshi, *Amorphous Magnetism* (CRC Press, Boca Raton, 1984), p. 88.
- ²¹L. G. C. Melo and A. D. Santos, *Mater. Sci. Forum* **302-303**, 219 (1999).
- ²²L. Kraus, *J. Magn. Magn. Mater.* **195**, 764 (1999).
- ²³K. R. Pirota, M. L. Sartorelli, M. Knobel, J. Gutierrez, and J. M. Barandiarán, *J. Magn. Magn. Mater.* **202**, 431 (1999).
- ²⁴R. L. Sommer and C. L. Chien, *Appl. Phys. Lett.* **67**, 857 (1995).
- ²⁵F. L. A. Machado and S. M. Rezende, *J. Appl. Phys.* **79**, 6558 (1996).
- ²⁶T. Uchiyama, K. Mohri, L. V. Panina, and K. Furuno, *IEEE Trans. Magn.* **MAG-31**, 3182 (1995).
- ²⁷M. Vázquez, G. V. Kurlyandskaya, J. L. Muñoz, A. Hernando, N. V. Dmitrieva, and V. A. Lukshina, *J. Phys. IV* **PR2**, 143 (1998).
- ²⁸R. L. Sommer and C. L. Chien, *J. Appl. Phys.* **79**, 5139 (1996).
- ²⁹G. V. Kurlyandskaya, J. M. García-Beneytez, M. Vázquez, J. P. Sinnecker, V. A. Lukshina, and A. P. Potapov, *J. Appl. Phys.* **83**, 6581 (1998).